A POLYGONAL GENERALIZED FINITE ELEMENT FOR UNIDIRECTIONAL COMPOSITE MICROSTRUCTURE SIMULATION

Murilo Sartorato
UNESP SP/Brazil
murilo.sartorato@unesp.br

unesp

Finep
INOVAÇÃO E PESQUISA

unesp
UNIVERSIDADE ESTADUAL PAULISTA
"JÚLIO DE MESQUITA FILHO"
Câmpus de São João da Boa Vista

INTRODUCTION / MOTIVATION

- UD composite microstructure RVE simulations are computationally expensive and generate large amount of degrees of freedom
- Microstructures create a natural **polygonal mesh** through the use of **Voronoi cells**
- Artificial Neural Networks training, optimization problems, and statistical analysis that need several realizations can **benefit from smaller models**

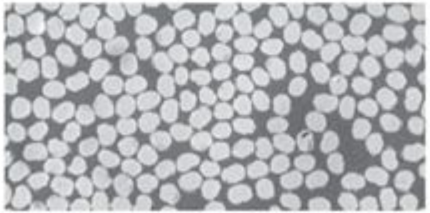

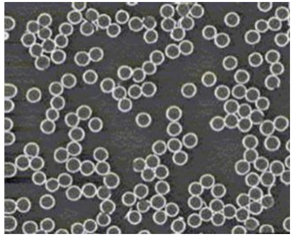

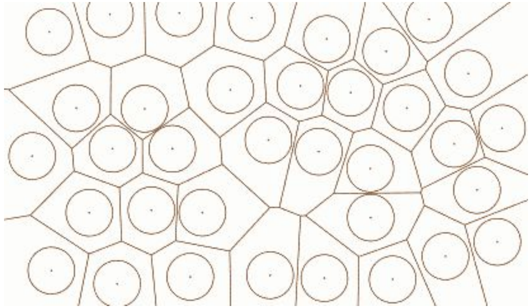

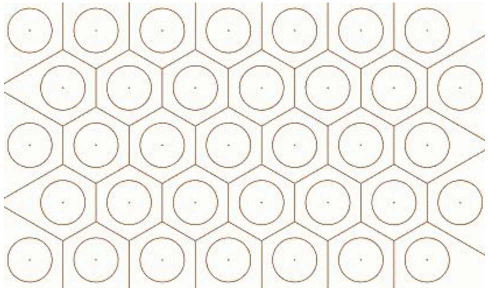

INTRODUCTION / MOTIVATION

- This work proposes a **Polygonal Finite Element** that accounts for the difference in properties between fiber and matrix and the corresponding stress concentration using **Generalized Finite Elements** techniques
- The main advantage over classic finite element solutions is a large decrease in the degrees of freedom of the model through the use of this enhanced-element

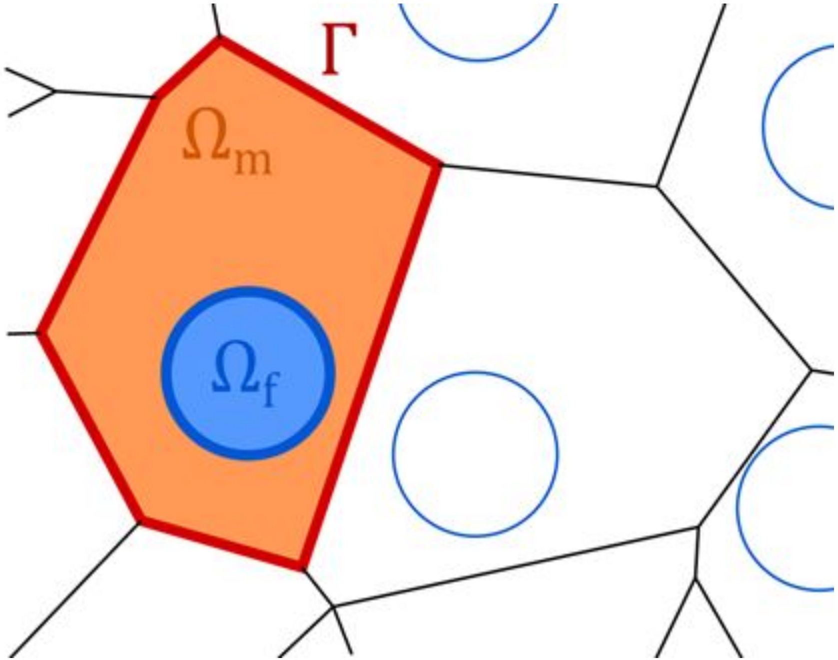

BASE SHAPE FUNCTIONS

- Wachspress functions

$$\varphi_n(x,y) = \frac{w_n(P)}{\sum_k w_k(P)}$$

$$w_k = \frac{A(Q_{k-1},\, Q_k,\, Q_{k+1})}{A(Q_{k-1},\, Q_k,\, P)\; A(Q_k,\, Q_{k+1},\, P)}$$

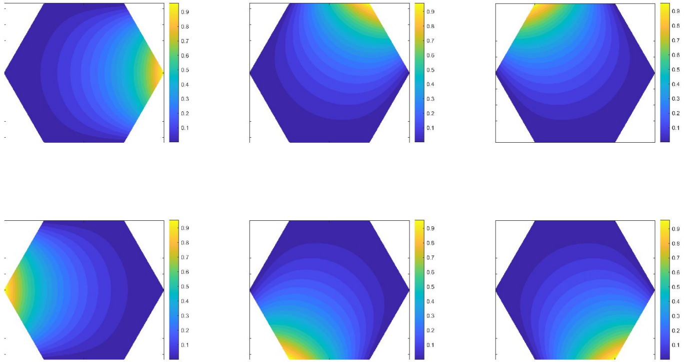

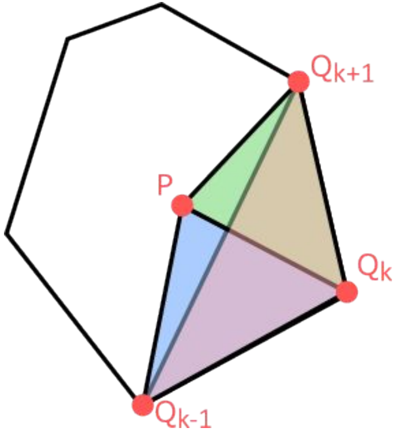

ENRICHMENT FUNCTIONS - GLOBAL

- Simple binomial polynomials of order $q=1..n$ centered on the element centroid
- Simulates/beaves as an h-enhancement of the element

$$\psi_{pq}^{global}(x,y) = (x-\bar{x})^p(y-\bar{y})^{q-p}$$

- Needed for the strain compatibility between elements and n-gons with fewer sides (3, 4 and 5)

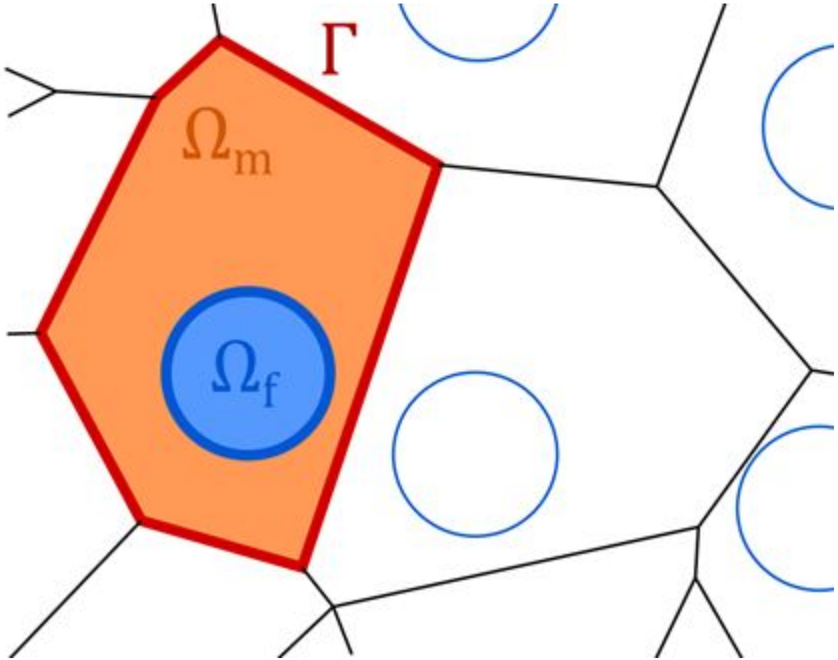

ENRICHMENT FUNCTIONS - STRESS

- Base radius gaussian functions centered on the points closest to the neighboring element for every n-side

$$\psi^s_{pn}(x,y) = \begin{cases} \exp\left(\frac{-\left(r - r_0^p\right)^2}{\sigma_n^2}\right), & if\,(x,y) \in \Omega_m \\ 0, & if\,(x,y) \in \Omega_f \end{cases}$$

- σ_p varies as percentages of δ starting from 10% up to 100% increasing logarithmically

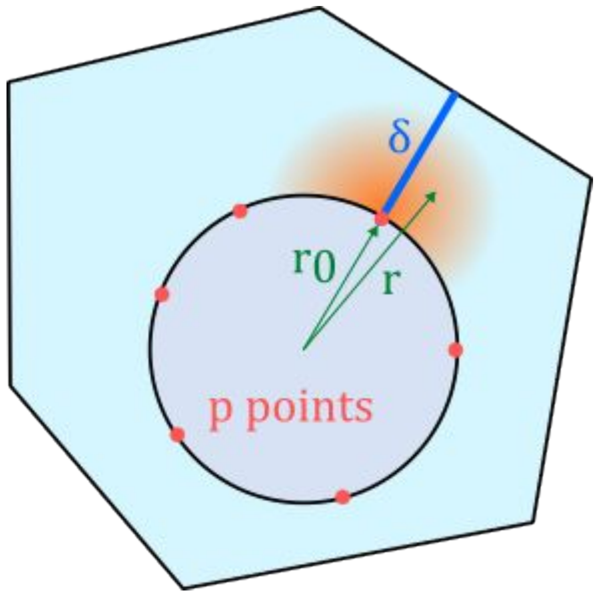

EXTRINSIC SHAPE FUNCTIONS

$$\phi(x,y) = \varphi(\xi,\,\eta) + \varphi(\xi,\,\eta)\psi^g(x,y) + \varphi(\xi,\,\eta)\psi^s(x,y)$$

$$\phi = \varphi \otimes \{1 \quad \psi^g \quad \psi^s\}$$

$$\nabla\phi = \nabla\varphi^T \otimes \{1 \quad \psi^g \quad \psi^s\} + \varphi \otimes \nabla\cdot\{1 \quad \psi^g \quad \psi^s\}^T$$

- Jacobian can easily be calculated as long as ψ_g and ψ_s are have closed forms and are C1
- Isoparametric mapping of coordinates and Ω_f is done through φ and an inversion through Newton-Raphson

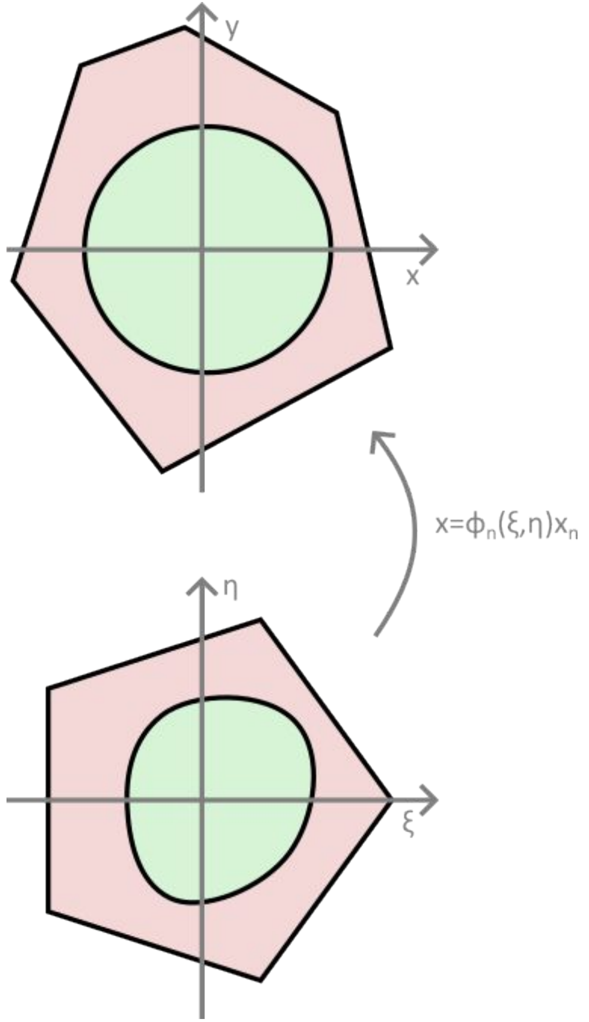

ELEMENT COMPATIBILITY

- The compatibility between neighboring elements is imposed through a penalization condition using Lagrange multipliers on every common side Γ
- The penalization is continuous using unidimensional cubic Hermite polynomials for the discretization of the penalizing forces

$$\delta\Pi_\Gamma = \delta\left(\oint_\Gamma \lambda_u \cdot \left(u_{\Gamma^-} - u_{\Gamma^+}\right) d\Gamma\right)$$

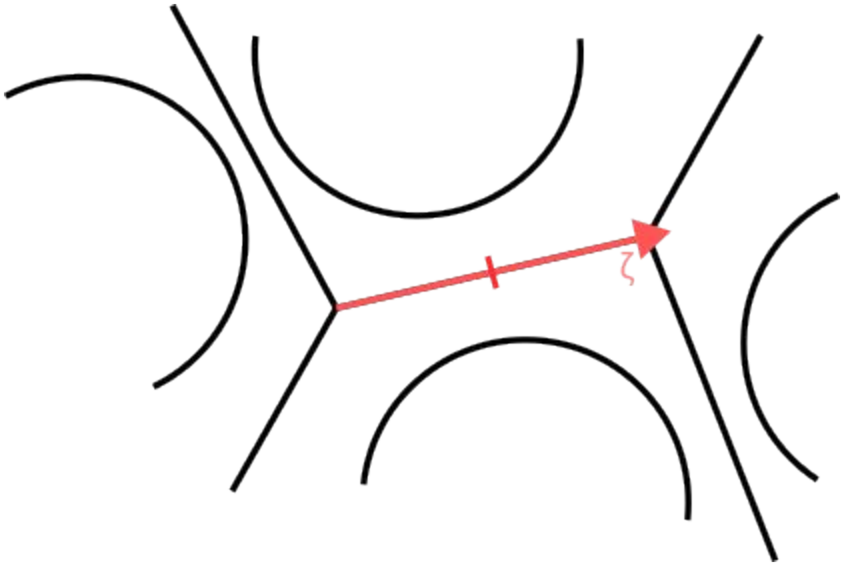

$$\chi = \left\{ \begin{matrix} \frac{1}{2}(1-\zeta) - \frac{1}{2}(1-\zeta^2) + \frac{1}{16}(-9\zeta^3 + \zeta^2 + 9\zeta - 1) \\ \frac{1}{2}(1+\zeta) - \frac{1}{2}(1-\zeta^2) + \frac{1}{16}(+9\zeta^3 + \zeta^2 - 9\zeta - 1) \\ (1-\zeta^2) + \frac{1}{16}(27\zeta^3 + 7\zeta^2 - 27\zeta - 7) \\ \frac{1}{16}(-27\zeta^3 - 9\zeta^2 + 27\zeta + 9) \end{matrix} \right\}$$

$$\lambda = \chi_p(\zeta)\lambda_p$$

GOVERNING EQUATIONS AND ELEMENTAL EQUILIBRIUM

- The variational of energy contribution from a single Voronoi cell is:

$$
\begin{aligned}
\delta\Pi_{elem} = \delta u^T \left(\int_{\Omega} B^T C_m B \, d\Omega + \int_{\Omega_f} B^T (C_f - C_m) B \, d\Omega \right) u + \\
+ \delta u^T \left(\oint_{\Gamma_i} \left(N^{\phi}_{\Gamma^-} - N^{\phi}_{\Gamma^+} \right)^T N^{\chi} d\Gamma_i \right) \lambda + \\
+ \delta \lambda^T \left(\oint_{\Gamma_i} N^{\chi T} \left(N^{\phi}_{\Gamma^-} - N^{\phi}_{\Gamma^+} \right) d\Gamma_i \right) u + \\
- \delta u^T \left(\int_{\Omega} N^{\phi^T} b \, d\Omega + \oint_{\Gamma_i} N^{\phi^T} t \, d\Gamma_i \right)
\end{aligned}
$$

- Three main integration domains exist: the whole n-gon element domain Ω, the fiber domain Ω_f and the boundaries Γ_i $i=1..n$

GOVERNING EQUATIONS AND ELEMENTAL EQUILIBRIUM

- In matrix form the elemental stiffnesses and coupling matrices are

$$K = \int_{\Omega} B^T C_m B \, d\Omega + \int_{\Omega_f} B^T (C_f - C_m) B \, d\Omega_f$$

$$L = \bigcup \oint_{\Gamma_i} N^{\chi^T} \left(N^{\phi}_{\Gamma^-} - N^{\phi}_{\Gamma^+} \right) d\Gamma_i$$

$$F = \int_{\Omega} N^{\phi^T} b \, d\Omega + \oint_{\Gamma_i} N^{\phi^T} t \, d\Gamma_i$$

$$\begin{bmatrix} K & L^T \\ L & \underline{0} \end{bmatrix} \begin{Bmatrix} u \\ \lambda \end{Bmatrix} = \begin{Bmatrix} F \\ \underline{0} \end{Bmatrix}$$

$$N^{\chi} = \begin{bmatrix} \chi \otimes \{1 \quad 0\} \\ \chi \otimes \{0 \quad 1\} \end{bmatrix}$$

$$N^{\phi} = \begin{bmatrix} \phi \otimes \{1 \quad 0\} \\ \phi \otimes \{0 \quad 1\} \end{bmatrix}$$

$$B = \begin{bmatrix} \phi_{,x} \otimes \{1 \quad 0\} \\ \phi_{,y} \otimes \{0 \quad 1\} \\ \phi_{,x} \otimes \{0 \quad 1\} + \phi_{,y} \otimes \{1 \quad 0\} \end{bmatrix}$$

- Three main integration domains exist: the whole n-gon element domain Ω, the fiber domain Ω_f and the boundaries Γ_i $i=1..n$

INTEGRATION STRATEGY

- Each element is divided into the two domain region Ω and Ω_f;
- The whole domain Ω is divided into triangles formed by two vertices and the fiber center
  - Each triangle is integrated using an adaptive Xiao-Gimbutas quadrature
- The fiber domain Ω_f is integrated using an adaptive King-Song quadrature
- Each side Γ_i is integrated using a classic Gauss-Legendre quadrature

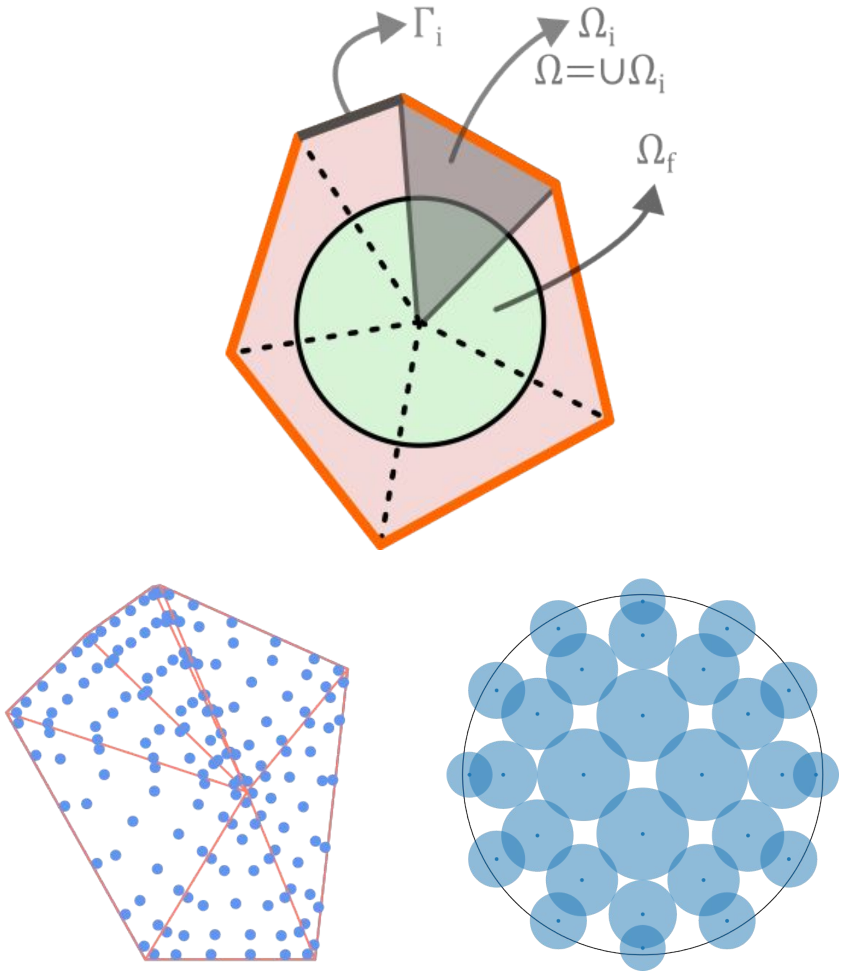

RVE GENERATION

- RVEs are generated from Weibull distributed fiber centers based microstructure images
- Fiber centers are identified through Python code and fit to a uniformly distributed hexagonal grid
- The distances are optimized using a re-annealing algorithm and the shape and scale parameters are obtained using a maximum likelihood estimation

$$k_{j+1}^{-1} = \frac{\sum_{i=1}^{n} x_i^{k_j} \ln x_i}{\sum_{i=1}^{n} x_i^{k_j}} - \frac{1}{n}\sum_{i=1}^{n} x_i^{k_j} \ln x_i, \quad \lambda_j = \frac{1}{n}\sum_{i=1}^{n} x_i^{k_j}$$

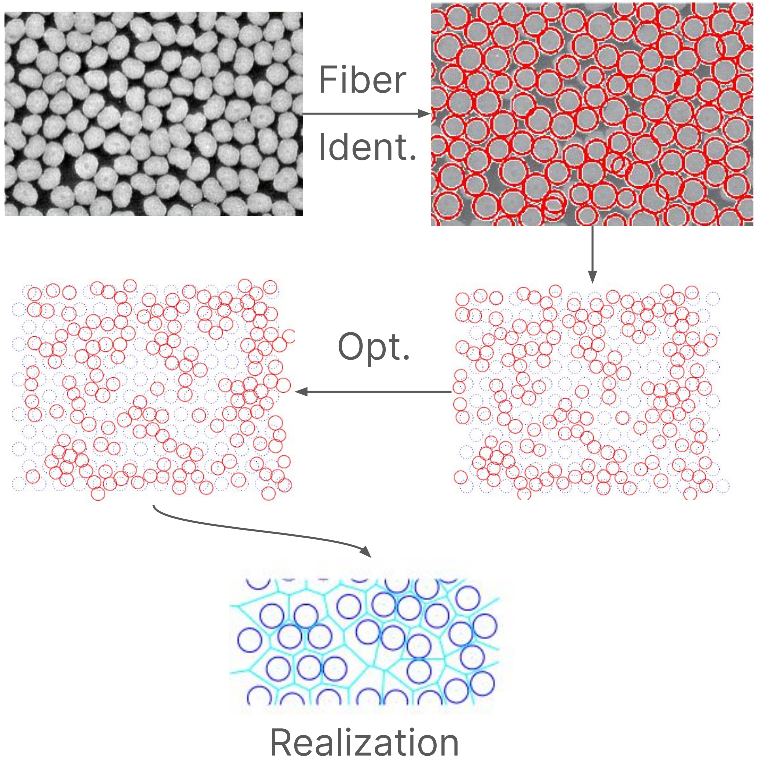

RVE GENERATION - EXAMPLES

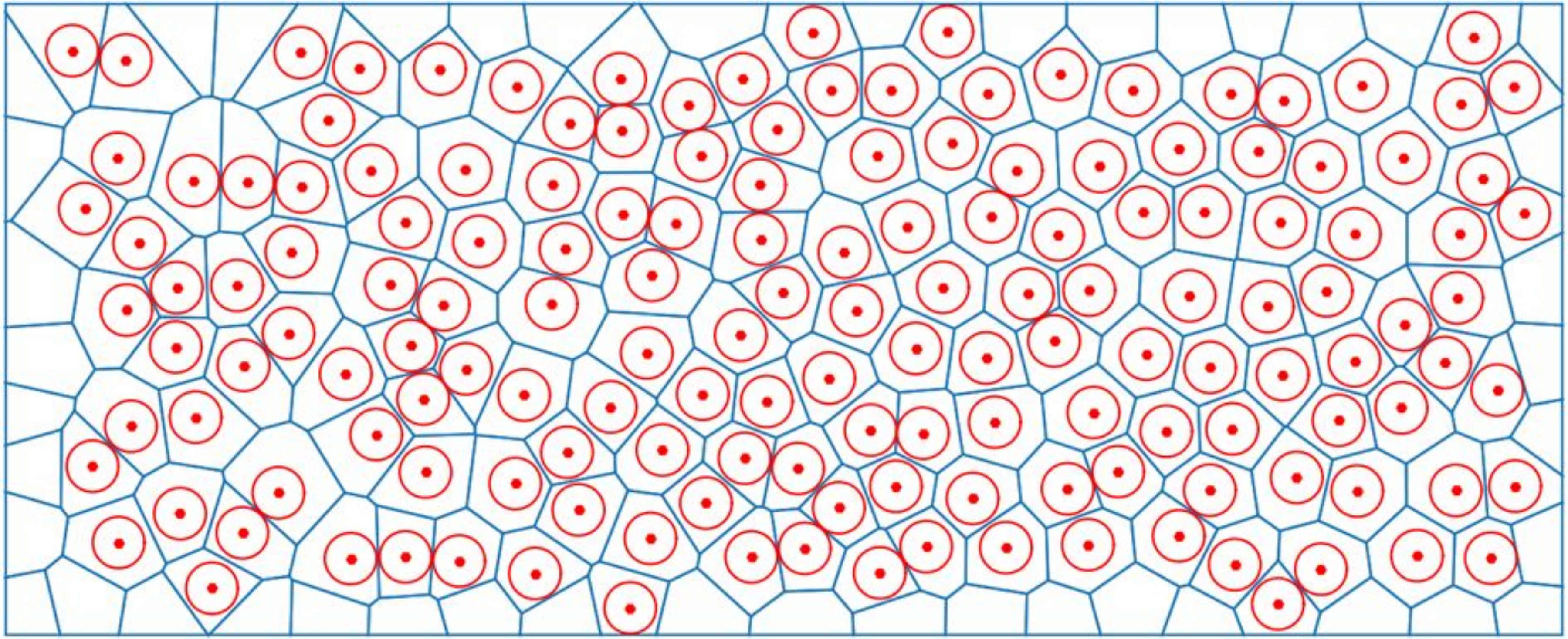

STUDY CASES

- Six study cases were created to study the efficiency and accuracy of the element comparing to a classic approach
  - Normal and shear loads applied to the RVE
  - Three levels of fiber density
    - $\nu_f \cong$ 40%, 60%, 68%

E_f [GPa]	ν_f []	E_m [GPa]	ν_m []
127	0.324	8.93	0.224

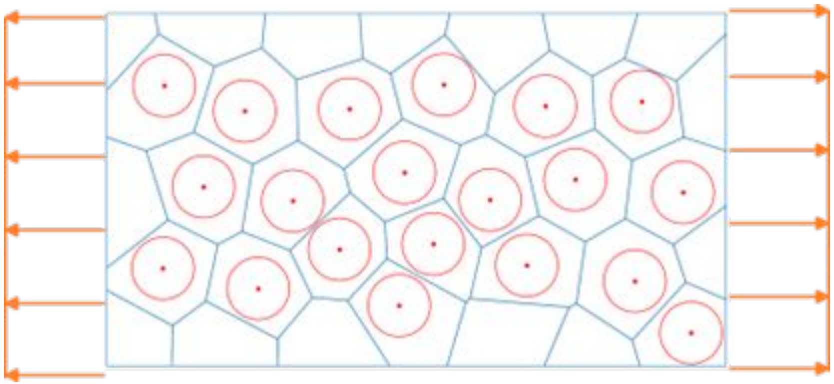

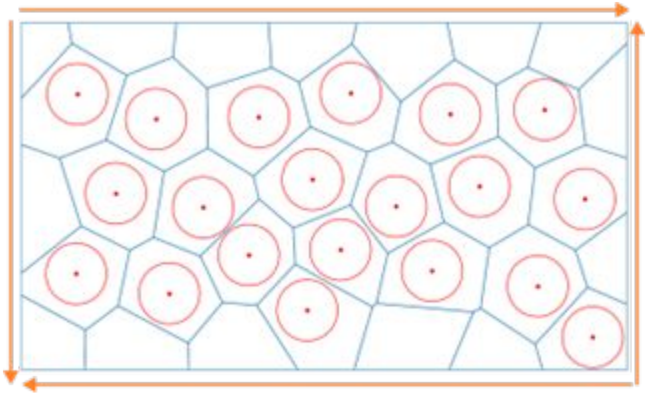

RESULTS

Volume fraction of fiber [%]	Solver	Number of degrees of freedom for convergence	Time [s]
40.75	Present Work	4423	7.636
	ABAQUS	5930564	1273.2
61.9	Present Work	4940	8.536
	ABAQUS	6349848	1402.3
68.87	Present Work	4780	7.838
	ABAQUS	6018381	1313.5

RESULTS

Volume fraction of fiber [%]	Load case	Solver	Maximum normalized displacement	% Difference	Average principal stress	Maximum principal stress	% Difference
40.75	Traction	Present Work	0.1034		14.026	519.34	
		Abaqus	0.1034	0.0000	14.026	451.8258	13.0000
	Shear	Present Work	0.145		19.669	728.2814	
		Abaqus	0.145	0.0000	19.2756	633.6048	13.0000
61.9	Traction	Present Work	0.0887		12.032	445.5073	
		Abaqus	0.0888	0.1127	11.8962	386.6903	13.2023
	Shear	Present Work	0.1043		14.1481	523.8604	
		Abaqus	0.1043	0.0000	13.8181	437.9473	16.4000
68.87	Traction	Present Work	0.0768		10.4178	385.738	
		Abaqus	0.0768	0.0000	10.2995	356.0362	7.7000
	Shear	Present Work	0.0993		13.4698	498.7472	
		Abaqus	0.0992	0.1007	13.424	459.8801	7.7929

CONCLUSIONS AND FUTURE WORKS

- The results obtained with the present methodology has showed perfectly accurate results for displacements and accurate enough results for stresses/strains in magnitude, but good at simulating position of maximum stresses when comparing to a commercial classic FEM solution, keeping an **average precision of 90%** for maximum values
- The number of **degrees of freedom in the models were reduced by several orders of magnitude**, increasing the applicability in ANN and optimization problems
- Future works on the influence of optic fiber sensors on damage and the optic-mechanical coupling through the vibration modes are possible

Acknowledgements

The author would like to thank Financiadora de Estudos e Projetos (FINEP) for partially funding the work through the grant MCTIC/FINEP/CT-INFRA Campi universitários regionais e novas universidades 02/2018;

Referência: 0527/18.

unesp

UNIVERSIDADE ESTADUAL PAULISTA
"JÚLIO DE MESQUITA FILHO"
Câmpus de São João da Boa Vista

Finep
INOVAÇÃO E PESQUISA